

1 **Plankton Reach New Heights in Effort to Avoid Predators**

2

3 **Brad J. Gemmell¹, Houshuo Jiang², J. Rudi Strickler³, Edward J. Buskey¹**

4 ¹University of Texas at Austin Marine Science Institute, ²Woods Hole Oceanographic Institution,
5 ³University of Wisconsin Milwaukee.

6

7 **ABSTRACT**

8 **The marine environment associated with the air-water interface (neuston) provides an**
9 **important food source to pelagic organisms where subsurface prey is limited. However,**
10 **studies on predator-prey interactions within this environment are lacking. Copepods are**
11 **known to produce strong escape jumps in response to predators but must contend with a**
12 **low Reynolds number environment where viscous forces limit escape distance. All previous**
13 **work on copepods interaction with predators has focused on a liquid environment. Here,**
14 **we describe a novel anti-predator behavior in two neustonic copepod species where**
15 **individuals frequently exit the water surface and travel many times their own body length**
16 **through air to avoid predators. Using both field recordings with natural predators and**
17 **high speed laboratory recordings we obtain detailed kinematics of this behavior, and**
18 **estimate energetic cost associated with this behavior. We demonstrate that despite losing**
19 **up to 88% of their initial kinetic energy, copepods which break the water surface travel**
20 **significantly further than escapes underwater and successfully exit the perceptive field of**
21 **the predator. This behavior provides an effective defense mechanism against subsurface**
22 **feeding visual predators and the results provide insight into trophic interactions within the**
23 **neustonic environment.**

24

25 **1. INTRODUCCION**

26 Copepods are one of the most abundant metazoans on the planet [1-2] and are known to
27 be important prey for fish [3-6] and other marine organisms [7-8]. The copepod's role in marine
28 food webs makes their behavioral adaptations to predation important to understand. The
29 neustonic environment consists of the upper few millimeters of water associated with the air-
30 water interface. This environment is often characterized by elevated biomass and numbers of
31 organisms relative to the water beneath [9] and provides food to higher trophic levels such as fish
32 [10]. Pontellid copepods are a ubiquitous group often found in neustonic environments and

33 adults are known to reside during daylight hours in the brightly lit surface water of coastal
34 oceans [11].

35 Many planktonic organisms residing in the photic zone have nearly transparent tissues
36 which are assumed to reduce conspicuousness to visual predators [12]. However, species which
37 live in close proximity to the water surface (neuston) are often highly pigmented, including
38 copepods [13]. Pigmentation in copepods has been demonstrated to reduce the effects of
39 damaging UV radiation [14-15] and may play a similar role in Pontellids. These copepods are
40 also large in comparison with many other copepod taxa [16]. This large size combined with
41 pigmentation makes these copepods more visually conspicuous and thus, should be preferred by
42 visual fish predators [17-18].

43 One of the mechanisms by which copepods are known to avoid fish predators is through
44 the use of powerful escape jumps [19-22]. These escape jumps are present throughout
45 development [23-24] and can generate speeds up to 800 mm s^{-1} and accelerations of up to 200 m
46 s^{-2} [20]. The interaction of copepods and their natural predators has been investigated in a liquid
47 medium [22, 25-26]. However aerial escapes have never been investigated for a planktonic
48 organism but may have significant ecological and evolutionary implications for the wide variety
49 of species that live and feed within the surface layer of the ocean.

50 Reports of copepods breaking through the water surface occurred as early as the late 19th
51 century [27]. The observer hypothesized that the leaps into the air and subsequent re-entry into
52 the water functioned as a mechanism to assist with molting, by jarring them loose from their old
53 exoskeleton. A later report of aerial copepod jumps proposed an anti-predator mechanism [28],
54 but the function of this behavior remained hypothetical.

55 Using field video recordings and high speed video in the laboratory, we demonstrate that
56 aerial jumps provide an effective escape mechanism in response to visual fish predators.
57 Kinematic analysis of this little known behavior reveals a significant energetic cost of breaking
58 the water surface, yet this aerial escape behavior still provides a net energy savings relative to an
59 escape performed solely underwater. These findings provide insight into how this group of
60 animals can be successful in a pelagic environment where they appear conspicuous and easily
61 targeted by visual predators.

62 **2. MATERIALS AND METHODS**

63 *a) Field recordings*

64 Field recordings were made using a hand-held video recorder at 30 frames s⁻¹ (Sony
65 Handycam CCD-TR3300) above the water surface. Recordings were edited in Adobe Premier
66 Pro to maximize distinction between copepods and the surrounding water by adjusting both
67 brightness and contrast. Two-dimensional escape kinematics in response to fish predators were
68 obtained using ImageJ v1.43 software. Statistical analysis for both laboratory and field
69 recordings were performed using Sigmaplot 11.0 (Systat Software Inc).

70 Field recordings of the copepod, *Anomalocera ornata* interacting with juvenile mullet
71 (*Mugil cephalus*) were performed for 15 min at the University of Texas Marine Science Institute
72 marina and escape responses from 89 individuals were obtained during analysis. The movement
73 of the camera required to follow individual fish interacting with copepods made simple size and
74 distance calibrations inappropriate. Instead, we captured and measured 22 of the juvenile *M.*
75 *cephalus* that were in the location of the video recordings and the resulting standard length of
76 24.2 mm (SD 1.96) was used to scale the video frames during kinematic analysis. This method
77 does not provide the finest spatial resolution but allows a reasonable approximation of both

78 distance and velocity. It should be noted that the calculated kinematic values represent minimum
79 estimates of both velocity and distance since recordings were based solely in an X-Y plane
80 normal to the camera lens so any Z component of motion was not accounted for. Therefore,
81 velocity and distance are likely underestimated but this effect is minimal for the laboratory
82 studies since the narrow (4 cm width) aquarium limited movement in the Z plane.

83 ***b) Laboratory recordings***

84 Copepods (*Labidocera aestiva*) were collected from inshore waters of the Northern Gulf
85 of Mexico (27° 50' 19" N 97° 3' 8" W) using a 0.5 m diameter plankton net (150 µm mesh).
86 Approximately 50 individuals were placed in a small, narrow rectangular acrylic aquarium
87 (20cm x 4cm x 20cm) filled to 50% capacity with filtered seawater. A high speed camera,
88 Redlake MotionMeter® model 1140-0003 equipped with a Nikon Nikkor 55-mm lens was used
89 to capture the escape behavior. Dark field illumination was provided by infrared light emitting
90 diodes (peak wavelength 890 nm). The copepod escape jumps were recorded at 250-500 frames
91 s⁻¹. After 10 recordings, copepods were replaced with 50 new animals to limit the probability of
92 recording the same animal multiple times.

93 Two camera positions were utilized during laboratory recordings. In position 1 the
94 camera was aligned with the aquarium so that the surface of the water was near the bottom of the
95 field of view in order to capture the entire aerial portion of the escape and 60 escapes were
96 recorded using this configuration. In position 2 the camera was oriented so that approximately
97 1/3rd of the field of view was below the surface of the water and 2/3rds were above the water
98 surface. This allowed determination of the copepod's speed as it broke the water's surface, the
99 contact angle to the surface and the trajectory through air. 24 escapes were recorded with this
100 configuration. The contact angle was determined at the instant contact was made at the water

101 surface, while the entire animal remained underwater. Using image analysis software (ImageJ)
102 we determined the angle using the water surface and the longitudinal central plane of the animal.
103 Recordings were performed in a darkroom and escape responses from the copepods were elicited
104 through a photic startle response by a rapid change in light intensity [29]. The subsequent escape
105 responses resulted in many copepods breaking the water's surface and traveling variable
106 distances through the air. Escapes in which more than 50% of the aerial trajectory was out of the
107 field of view were not used for analysis. In cases where only a smaller portion (less than 50%) of
108 the escape traveled beyond the field of view, the maximal distance was extrapolated using
109 Vogel's model for an object in free fall [30]. This was required for 19 of the 60 escapes used in
110 our analysis.

111 *c) Data analysis*

112 To compare the kinematic results obtained from both ImageJ v1.43 software and Celltrak
113 v1.5 motion analysis software, data was log transformed and checked for normality using a
114 Shapiro-Wilk test. A one-way analysis of variance (ANOVA) was performed for both total
115 horizontal distance and maximum velocity.

116 We used the following equation to estimate the net kinetic energy loss (ΔK) incurred
117 from a copepod breaking the water surface:

$$118 \quad \Delta K = 0.5 m_{\text{copepod}} (U_0^2 - U_1^2) \quad (1)$$

119 where m_{copepod} is the body mass of the copepod, U_0 is the copepod velocity at the moment just
120 before the copepod starts to break the water surface, and U_1 is the copepod velocity at the
121 moment right after the copepod becomes completely airborne. $m_{\text{copepod}} = \rho_{\text{copepod}} \times V_{\text{copepod}}$, where
122 ρ_{copepod} is the mass density of the copepod (approximately equal to the mass density of the

123 seawater, ρ_{seawater}), and V_{copepod} is the copepod body volume. V_{copepod} is calculated as $4/3\pi\eta^2a^3$,
124 where a is half the prosome length, η the copepod aspect ratio, and assuming the shape of a
125 prolate spheroid with the long axis equal to the prosome length, $2a$, and the short axis equal to
126 $\eta \times 2a$.

127 Here, we estimate three likely contributions to this energy loss:

128 (1) The loss due to the water drag can be estimated as:

$$129 \quad \Delta K_1 = 0.25 C_d \rho_{\text{seawater}} U_0^2 S_e d_e \quad (2)$$

130 where C_d is the drag coefficient of the equivalent sphere having the same volume as that of the
131 copepod body, S_e is the cross-sectional area of the equivalent sphere, and d_e is the diameter of the
132 equivalent sphere. We estimate this energy loss during breaking the water surface (very short
133 time scale) as the average between the moment the animal makes contact with the surface (fully
134 underwater), and moment the animal fully breaks free of the surface (fully in air). Here, we
135 assume that the drag acting on the copepod when it just starts to break the water surface is $0.5 C_d$
136 $\rho_{\text{seawater}} U_0^2 S_e$, and the drag acting on the copepod when it just leaves the water surface to
137 become completely airborne is $0.5 C_d \rho_{\text{air}} U_1^2 S_e$, where ρ_{air} is the mass density of air. Because ρ_{air}
138 $\ll \rho_{\text{seawater}}$, the average drag for this short time interval is approximately $0.25 C_d \rho_{\text{seawater}} U_0^2 S_e$.
139 The average drag multiplied by the distance traveled, d_e , leads to Equation (2). C_d is calculated
140 based on the Reynolds number $\text{Re} = U_0 d_e / \nu_{\text{seawater}}$, where ν_{seawater} is the kinematic viscosity of
141 the seawater. Although we are not sure about the applicability of the commonly used drag law,
142 Equation (2) should give upper bound estimation of the energy loss due to the water drag.

143 (2) The loss due to the increase of the gravitational potential energy of the copepod body
144 estimated as:

145 $\Delta K_2 = m_{\text{copepod}} g d_e \cos(\alpha)$ (3)

146 where g is acceleration due to gravity, and α is the exit angle (figure S1).

147 (3) The loss due to overcoming the surface tension:

148 $\Delta K_3 = \sigma A_{\text{copepod}} \cos(\theta)$ (4)

149 where σ ($= 0.075 \text{ N m}^{-1}$) is the surface tension for the seawater-air interface, A_{copepod} is the
150 surface area of the copepod, and θ is the contact angle between the copepod body and the
151 seawater surface. Here, we assume that the energy loss is due to the copepod surface condition
152 changing from interfacing with seawater to interfacing with air, i.e.

153 $\Delta K_3 = (\sigma_{\text{copepod-air}} - \sigma_{\text{copepod-seawater}}) A_{\text{copepod}}$, where $\sigma_{\text{copepod-air}}$ and $\sigma_{\text{copepod-seawater}}$ are the surface
154 energies associated with the copepod-air and copepod-seawater interfaces, respectively. Using
155 Young's law for the contact angle, i.e. $\sigma_{\text{copepod-air}} = \sigma_{\text{copepod-seawater}} + \sigma \cos(\theta)$ [31], we obtain
156 Equation (4).

157 3. RESULTS

158 Field video recordings captured the copepod *Anomalocera ornata* (prosome length 2.5-
159 3.1 mm) in the presence of small plankton feeding fish (juvenile *Mugil cephalus*) within inshore
160 waters of the Northwestern Gulf of Mexico. The escape behavior was stimulated by the approach
161 of the predatory fish, *M. cephalus*, (figure 1) and consisted of an airborne leap covering a
162 horizontal distance of 80 ± 30 mm (N= 89), with maximum distances of up to 170 mm observed
163 (see data supplement for video of this behavior). On average, the copepods travelled over 40
164 times their own body length and 3.4 times the body length of the fish predator (mean standard
165 length 24.2mm). The maximum aerial velocity achieved during these escapes was 890 ± 200 mm

166 s⁻¹ and average velocities over the entire escape were 660 ±150 mm s⁻¹ (figure 2a). Only 1 of the
167 89 observed escapes resulted in multiple attacks by the same fish.

168 A smaller Pontellid copepod (prosome length 1.8-2.0 mm), *Labidocera aestiva*, was
169 stimulated to perform escape jumps in the laboratory using a photic startle response and the
170 escapes were recorded with a high speed video camera at 250-500 frames s⁻¹(see data supplement
171 for video of this behavior). This species swam approximately 0-40 mm below the water's surface
172 until stimulated to escape. We found that maximum aerial velocity of the copepods after they
173 broke the water's surface to be 630 ±150 mm s⁻¹. This was significantly lower (P = <0.001) than
174 velocities produced by *A. ornata* and also resulted in significantly lower (P = <0.001) horizontal
175 escape distances (figure 2a). *Labidocera aestiva* was able to attain heights over 60 mm above the
176 water's surface and up to 76 mm in distance from the exit point in the water. However, the mean
177 horizontal distance travelled during escapes through air was 16.0 ±14.1 mm. It is interesting to
178 note that in most cases rotation was imparted on the animal as it broke the surface (see
179 supplemental video). In some cases the rotation was estimated in excess of 45,000 degrees s⁻¹
180 (7500 rpm). The underwater portion of the escapes for *L. aestiva* yielded maximum velocities of
181 1036 ±121 mm s⁻¹ which is significantly greater (P = <0.001) than maximum velocities observed
182 after breaking the surface.

183 The results of a correlation analysis between horizontal escape distance and maximum
184 aerial velocity for *A. ornata* exhibited a moderate relationship (R²= 0.36) (figure 2b). The same
185 analysis performed for *L. aestiva* exhibited virtually no correlation between horizontal escape
186 distance and maximum aerial velocity (R²= 0.04) (figure 2c). Notably, swimming pattern and
187 orientation of the two species relative to the water surface before escape is also different (figure
188 3). *L. aestiva* was observed to swim freely below the water surface using an intermittent

189 (cruising-sinking) swimming pattern. During the cruising phase, the copepod was oriented
190 randomly to the water surface but during sinking, *L. aestiva* was consistently observed to orient
191 with its anterior end towards the water surface. *A. ornata* exhibited a cruising swimming pattern
192 and was consistently oriented with its ventral side facing downwards (away from the surface)
193 and the dorsal side of the animal at the water surface.

194 When high speed recordings during the aerial portion of an escape jump of *L. aestiva* are
195 compared to a model of biological projectiles [29] the copepod acts as a ballistic object in free-
196 fall (figure 4a). Using data from both 500 fps and 250 fps observations, we estimate that 58-
197 88% of the kinetic energy at the moment when the copepod starts to break the water surface will
198 be lost for breaking the water surface (figure 4b). Among the total loss (fit to the data), 61-67%
199 is due to overcoming the water drag force (i.e. ΔK_1), the contribution from increases of
200 gravitational potential energy (ΔK_2) is negligible, and the loss due to overcoming the surface
201 tension (ΔK_3) is 33-39%. When a similar calculation is made for adult flying fish which are
202 orders of magnitude larger than Pontellid copepods, yet produce a functionally analogous
203 behavior, the cost of breaking the surface is $< 0.07\%$ of the kinetic energy possessed at the
204 moment when the fish starts to break the water surface.

205 **4. DISCUSSION**

206 Large scale movement of copepods that reside in the neustonic surface layer of the ocean
207 is often subject to surface currents. They have been observed to accumulate at oceanic frontal
208 boundaries [32] where small predatory fish are also more abundant [33]. Thus, successful
209 predator evasion is essential to the copepod's survival. However being confined at the surface
210 limits escape ability and predators have been observed using the water surface to aid in prey
211 capture [34]. The ability of some Pontellid copepods to break the water surface provides

212 advantages over escapes which occur solely underwater. First, exiting the perceptive field of a
213 predator and re-entering at a random location reduces the chance of continued pursuit and the 80
214 ± 30 mm horizontal escape distance observed for *A. ornata* is well beyond the perceptive distance
215 determined for fish of the similar length to *C. mugil* [35]. Second, for a copepod to achieve a
216 similar escape distance solely underwater, it would have to expend ~ 20 times more mechanical
217 energy, therefore a significant energetic savings exists by jumping into air.

218 The underwater velocity is higher than maximum velocities reported for other similarly
219 sized copepods [20] which facilitate these small organisms breaking the water surface. However,
220 the mode in which the two species of copepods exit the water is different (figure 3). *A. ornata*
221 consistently swims with its dorsal side at the water surface while the anterior end of *L. aestiva*
222 was generally directed toward the surface but was observed to swim at many orientations just
223 below the surface. This may explain why *L. aestiva* exhibits a lower correlation between
224 maximum aerial velocity and horizontal distance than *A. ornata* (figure 2b, c).

225 Considering a single stroke escape jump that occurs completely underwater, the copepod
226 achieves its peak velocity approximately at the end of the power stroke of the swimming legs.
227 During the power stroke, the copepod travels a distance nL , where L is the prosome length and n
228 $\sim 1-2$ [21]. Upon completion of the power stroke, the copepod rapidly decelerates due to drag
229 forces but maintains enough inertia to move forward another distance of $\sim nL$ until coming to
230 rest. The present observations show that copepods, via a one-kick jump, can break the surface of
231 the water (see supplemental video) and peak velocity (U_0) is obtained just before breaking the
232 surface. At the moment when the animal becomes completely airborne it travels at a velocity
233 (U_1), which is significantly smaller than U_0 . In other words, there is a net kinetic energy loss

234 (figure 4b). The net kinetic energy loss (ΔK) incurred during the copepod *Labidocera aestiva*
235 breaking the water surface is 58-88%.

236 This energy loss, however, is compensated for by increased escape distance. After
237 becoming airborne, the copepod can travel significantly farther than nL (i.e. the distance it
238 otherwise travels underwater) because it now experiences the air mass density, which is ~ 850
239 times smaller than the mass density of seawater. Therefore, the copepod will experience less drag
240 resulting in increased distance. There is no propulsive force exerted by the copepod after it
241 becomes airborne, and the copepod undergoes ballistic motion because of gravity (and the air
242 drag force) (figure 4a).

243 Our field observations show that copepods can effectively use aerial escapes as an anti-
244 predator mechanism. By leaving the perceptive environment of the visual fish predators and re-
245 entering the water up to 170 mm (≈ 60 body lengths) away from the attack site, a copepod can
246 utilize this effective strategy which appears analogous to that of some larger organisms (e.g.
247 flying fish). An important difference, however, is that all species known to perform similar types
248 of behavior are orders of magnitude larger than copepods. This means that copepods must
249 contend with the reduced inertial forces (lower Reynolds number) and a greater proportion of the
250 total energy dedicated to break the surface tension of water.

251 Consider the case of a flying fish. We calculate that flying fish lose $<0.07\%$ of their
252 overall kinetic energy breaking the surface tension compared to 33-39% in the case of the
253 copepod, despite a greater magnitude of energy loss (due to larger surface area) than copepods.
254 This is due to the fact that flying fish possess orders of magnitude more kinetic energy upon
255 contact with the water surface because of much greater mass and underwater speeds of $\approx 10 \text{ m s}^{-1}$
256 [36], compared to $\approx 1 \text{ m s}^{-1}$ in copepods. However, it should be noted that although aerial escapes

257 in larger, heavier aquatic animals lose almost no kinetic energy from surface tension effects,
258 horizontal distances in terms of body length (for animals exhibiting ballistic aerial motion) are
259 much shorter [37]. Thus, what appears to be a disadvantage of small mass (e.g. losing significant
260 proportion of kinetic energy) can translate into an advantage: once the water surface is broken,
261 the copepod travels disproportionately farther than larger animals (with ballistic flight paths). The
262 major reason for this is that the copepod has the ability to generate and maintain a
263 disproportionately large air-entry velocity (relative to body length) compared to larger animals. A
264 secondary reason might be that the flying copepod experiences smaller air drag-induced
265 deceleration than larger animals. Therefore ballistic aerial escape paths can be effective in
266 pelagic ecosystems when the animal (and predator) is small, but are unlikely to carry a larger
267 animal out of the perceptive range of their predator. Instead, specialized structures and behavior
268 such as those observed in flying fish are required to extend horizontal distance above water.

269 Because escapes are energetically costly [38-40], a copepod's fitness can be reduced even
270 without being captured by a predator. It therefore benefits the copepod to balance predation risk
271 and energy cost by avoiding unnecessary escapes. To avoid pursuit or multiple attacks from a
272 predator, copepods must travel to a distance outside of the perceptive range of the predator.
273 During an escape, a copepod travels approximately 1-2 times its prosome length per stroke
274 (calculated from [21]). For the Pontellid copepods this would result in a distance of 2-6 mm per
275 stroke. However, even small fish can perceive prey at least 10 mm away [35, 41] thus; multiple
276 escape jumps are required for a copepod to exit the predator's perceptive field. Therefore, if an
277 escape occurs in air rather than water, reduced drag forces can extend escape distance. This can
278 transport a copepod further from a predator with a single escape jump, than with multiple jumps

279 in an aqueous environment, resulting in net energy savings. They also return to the water in an
280 unpredictable location making pursuit from the predators unlikely.

281 Finally, the Pontellid copepods may have special adaptations to make it easier for them to
282 jump out of the water: One possible adaptation is that the body surface of those copepod species
283 that do perform such air-entering jumps is less wettable than other copepods or crustaceans in
284 general and thus, their surface properties may be essential for their unusual capability of
285 breaking the water surface. Our kinetic energy budget calculation suggests that if the surface
286 tension is not altered during the breaking of the surface (i.e. a constant $\sigma = 0.075 \text{ N m}^{-1}$), in order
287 to maintain a useful level of kinetic energy after breaking the surface the copepod body surface
288 has to be hydrophobic, i.e. much larger contact angle in the $68\text{-}81^\circ$ range [Fig. 4b; calculated
289 according to Equation (4)]. Another suspected adaptation may be that the copepods inject
290 chemicals during breaking of the surface to reduce the surface tension by 3-6 times, and
291 therefore a useful level of air-entry kinetic energy can still be maintained even when the contact
292 angle remains similar to published measurements for other crustaceans in the range of below 20°
293 [42]. Further investigation is required to find out if these adaptations indeed exist. Nevertheless,
294 unusual morphological structures are known to exist on the dorsal side of Pontellid copepods
295 [43], which might contribute to making the copepod body surface less wettable. However, these
296 morphological structures make up only a small part of the animal's total surface and
297 alternatively, pores specialized for secretion onto the body surface exist in Pontellids [44].
298 Similar pores with currently unknown function may also be involved in secreting substances
299 presumably to alter surface properties or surface tension of water immediately surrounding the
300 animal. Regardless of the mechanism, escaping through air appears to be an effective strategy to
301 not only avoid and survive attacks from predators by temporarily exiting the liquid environment

302 and exiting the predator's perceptive field, but also to conserve energy during escapes, providing
303 a competitive advantage for Pontellid copepods in the neustonic environment.

304

305 **Acknowledgements:**

306 This work was supported by grants from the National Science Foundation, USA to EJB (NSF
307 OCE-0452159), to HJ (NSF OCE-1129496). C. Brown assisted BJG with collection and E.
308 Hing-Fay maintained copepods for JRS.

309

310 **Figure legends:**

311

312 Figure 1. Representative diagram showing the copepod, *Anomalocera ornata*, response to the
313 approach of a planktivorous fish predator (juvenile *Mugil cephalus*). The fish swims in a
314 random cruising pattern just below the water surface until visually encountering a
315 copepod. a) Once located visually, the fish swims toward the copepod and attempts to
316 ingest it. b) The approach of the fish alerts the copepod to the presence of a potential
317 predator and the copepod responds with an aerial leap. c) The copepod travels many
318 times its own body length and significantly further than a single escape underwater to exit
319 the perceptive field of the predator. d) Once the copepod re-enters the water it resumes
320 swimming at the surface. Note: Not drawn to scale.

321

322 Figure 2. a) Relationship between horizontal distance and maximum aerial velocity for two
323 species of copepods during airborne escapes. *Anomalocera ornata* exhibits a significantly
324 greater horizontal distance ($P = <0.001$, $\alpha = 0.050$: 1.000 One-way ANOVA) and aerial
325 velocity ($P = <0.001$, $\alpha = 0.050$: 1.000 One-way ANOVA) than *Labidocera aestiva*. The
326 larger copepod, *A. ornata*, is able to travel proportionally further per unit energy. Note:
327 maximum aerial velocity was obtained at the moment the animal fully exited the water
328 surface. Error bars represent Standard Deviation. b) Regression plot for *A. ornata* ($R^2 =$
329 0.36) and c) *L. aestiva* ($R^2 = 0.04$), where *A. ornata* shows a stronger correlation of
330 velocity with distance.

331

332 Figure 3. Two observed techniques utilized by neustonic copepods to break through surface
333 tension of seawater during aerial escape responses. a) *Labidocera aestiva* swims below
334 the surface and is often oriented with the anterior portion of its body toward the water
335 surface (1). b) *Anamolcera ornata* swims at the air-water interface with its dorsal side
336 facing the surface and ventral side facing downwards (1). After being stimulated to
337 perform an escape, swimming appendages (pereiopods) of both species beat sequentially
338 as antennae fold against the body as the animal is propelled forward (2). As the animals
339 accelerate, the increase in kinetic energy allows the body to overcome surface tension
340 forces and travel through the air (3).

341

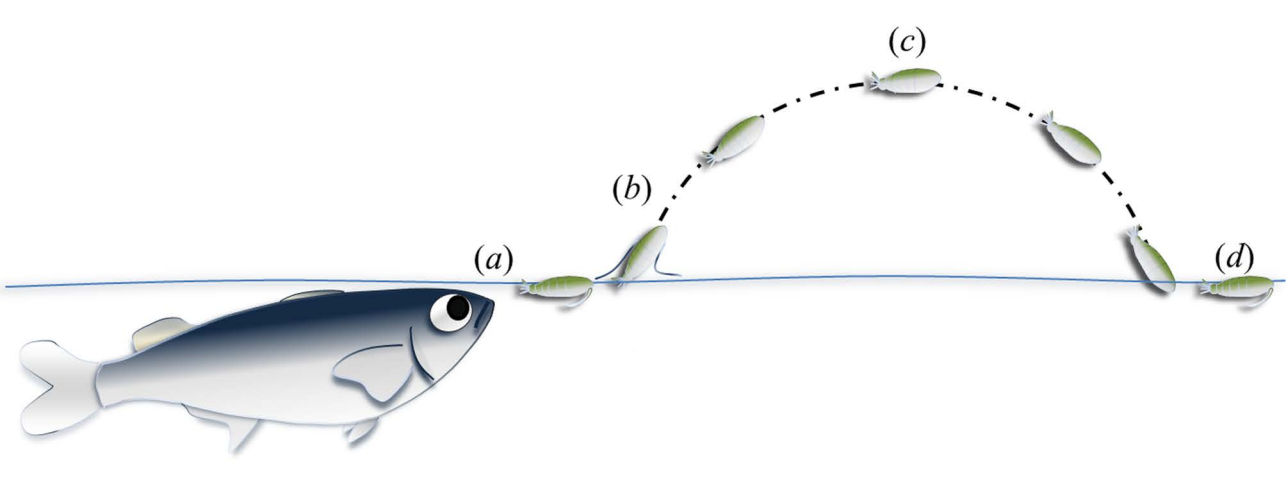
342 Figure 4. a) Observed copepod trajectory during airborne versus a ballistic/free-fall model
343 prediction. b) Kinetic energy loss as a function of the copepod (maximum) speed below
344 water surface. The squares label the data obtained via 500-frames-per-second video
345 recording, and the triangles label the data obtained via 250-frames-per-second video
346 recording. The solid green line is a fit to the data ($\Delta K = 1.26 \times 10^{-7} U_0^2$, where U_0 is the
347 copepod speed below water surface). The solid blue line is the contribution to the kinetic
348 energy loss due to water drag. The solid red line is the difference between the green line
349 and the blue line. The 2 dashed horizontal lines represent, respectively, the work needed
350 to overcome the surface tension in order for the copepod to be airborne for 2 assumed
351 receding contact angles between the copepod and the seawater interface [calculated from
352 Equation (4) for a constant $\sigma = 0.075 \text{ N m}^{-1}$]. Note that the red line is bounded between
353 these 2 dashed horizontal lines. Copepod prosome length = 1.8 mm, and aspect ratio =
354 0.32.

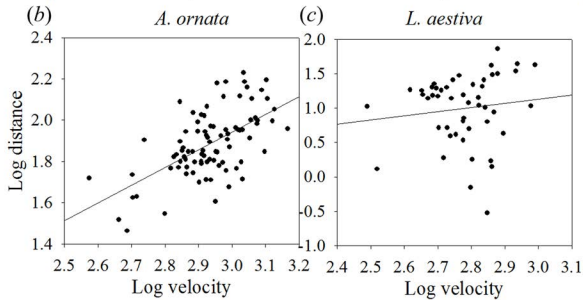
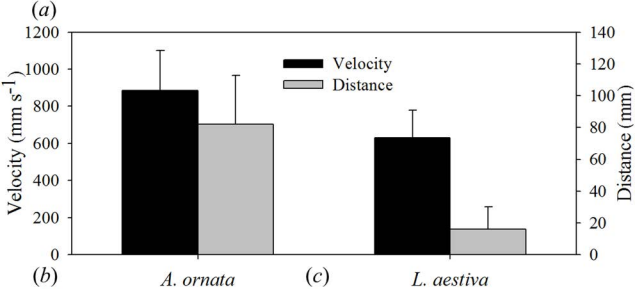
References:

- 356 1. Humes, A. G. 1994 How many copepods? *Hydrobiologia*, **292/293**, 1–7. (DOI
357 10.1007/BF00229916)
- 358 2. Turner, J. T. 2004. The importance of small planktonic copepods and their roles in
359 pelagic marine food webs. *Zool. Stud.* **43**, 255–266.
- 360 3. Govoni, J. J. & Chester, A. J. 1990. Diet composition of larval *Leiostomus xanthurus* in
361 and about the Mississippi River plume. *J. Plankton Res.* **12**, 819–830. (DOI
362 10.1093/plankt/12.4.819)
- 363 4. Anderson, J. T. 1995. Feeding ecology and condition of larval and pelagic juvenile
364 redbfish *Sebastes spp.* *Mar. Ecol. Prog. Ser.* **104**, 211–226.
- 365 5. Hillgruber, N., Haldorson, L. J. & Paul, A. J. 1995. Feeding selectivity of larval walleye
366 pollock *Theragra chalcogramma* in the oceanic domain of the Bering Sea. *Mar. Ecol.*
367 *Prog. Ser.* **120**, 1–10. (DOI 10.3354/meps120001)
- 368 6. Conway, D., Coombs, S. H. & Smith, C. 1998. Feeding of anchovy *Engraulis*
369 *encrasicolus* larvae in the northwestern Adriatic Sea in response to changing
370 hydrobiological conditions. *Mar. Ecol. Prog. Ser.* **175**, 35–49. (DOI
371 10.3354/meps175035)
- 372 7. Costello, J. H. & Colin, S. P. 1994. Morphology, fluid motion and predation by the
373 scyphomedusa *Aurelia aurita*. *Mar Biol.* **121**, 327–334. (DOI 10.1007/BF00346741)
- 374 8. Oresland, V. 1995. Winter population structure and feeding of the chaetognath *Eukrohnia*
375 *hamate* and the copepod *Euchaeta antarctica* in Gerlache Strait, Antarctic Peninsula.
376 *Mar. Ecol. Prog. Ser.* **119**, 77–86. (DOI 10.3354/meps119077)
- 377 9. Sieburth, J. M., P.-J. Willis, K. M. Johnson, C. M. Burney, D. M. Lavoie, K. R. Hinga, D.
378 A. Carson, F. W. French III, P. W. Johnson, & P. G. Dairs. 1976. Dissolved organic
379 matter and heterotrophic microneuston in the surface microlayers of the North Atlantic.
380 *Science* **194**, 1415–1418. (DOI 10.1126/science.194.4272.1415)
- 381 10. Brodeur, R. D. 1989. Neustonic feeding by juvenile salmonids in coastal waters of the
382 Northeast Pacific. *Can. J. Zool.* **67**, 1995–2007. (DOI 10.1139/z89-284)
- 383 11. Tester, P. A., Cohen, J. H. & Cervetto, G. 2004. Reverse vertical migration and
384 hydrographic distribution of *Anomalocera ornata* (Copepoda: Pontellidae) in the US
385 south Atlantic bight. *Mar. Ecol. Prog. Ser.* **268**, 195–203. (DOI 10.3354/meps268195)
- 386 12. Hansson, L. A. 2000. Induced pigmentation in zooplankton: a trade-off between threats
387 from predation and ultraviolet radiation. *Proc. R. Soc. Lond.* **267**, 2327–2332. (DOI
388 10.1098/rspb.2000.1287)
- 389 13. Herring, P. J. 1965. Blue pigment of a surface-living oceanic copepod. *Nature.* **205**, 103–
390 104. (DOI 10.1038/205103a0)
- 391 14. Byron, E. R. 1982. The adaptive significance of Calanoid copepod pigmentation: a
392 comparative & experimental analysis. *Ecology* **63**, 1871–1886. (DOI 10.2307/1940127)
- 393 15. Hansson, L. A., Hylander, S. & Sommaruga, R. 2007. Escape from UV threats in
394 zooplankton: A cocktail of behavior and protective pigmentation. *Ecology* **88**, 1932–
395 1939. DOI 10.1890/06-2038.1)
- 396 16. Mauchline, J. 1998. *The Biology of Calanoid Copepods. Advances in Marine Biology.*
397 Vol. 33. Academic Press, San Diego.
- 398 17. Brooks, J. L. & Dodson, D. I. 1965. Predation, body size, and composition of the
399 plankton. *Science* **150**, 28–35. (DOI 10.1126/science.150.3692.28)

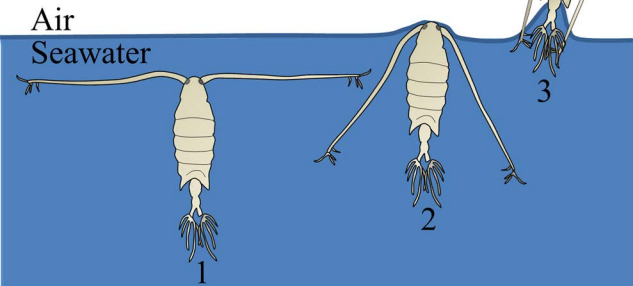
- 400 18. Morgan, S. G. & Christy, J. H. 1996. Survival of marine larvae under the countervailing
401 selective pressures of photodamage and predation. *Limnol. Oceanogr.* **41**, 498-504. (DOI
402 10.4319/lo.1996.41.3.0498)
- 403 19. Buskey, E. J., Lenz, P. H. & Hartline, D. K. 2002. Escape behavior of copepods in
404 response to hydrodynamic disturbances: high speed video analysis. *Mar. Ecol. Prog. Ser.*
405 **235**, 135–146. (DOI 10.3354/meps235135)
- 406 20. Lenz, P. H., Hower, A. E. & Hartline, D. K. 2004. Force production during pereopod
407 power strokes in *Calanus finmarchicus*. *J. Mar. Systems.* **49**, 133-144. (DOI
408 doi:10.1016/j.jmarsys.2003.05.006)
- 409 21. Waggett, R. J. & Buskey, E. J. 2007. Calanoid copepod escape behavior in response to a
410 visual predator. *Mar. Biol.* **150**, 599–607. (DOI 10.1007/s00227-006-0384-3)
- 411 22. Viitasalo, M., Kiørboe, T., Flinkman, J., Pedersen, L. W. & Visser, A. W. 1998.
412 Predation vulnerability of planktonic copepods: consequences of predator foraging
413 strategies and prey sensory abilities. *Mar. Ecol. Prog. Ser.* **175**, 129–142. (DOI
414 10.3354/meps175129)
- 415 23. Buskey, E. J. 1994. Factors affecting feeding selectivity of visual predators on the
416 copepod *Acartia tonsa*: locomotion, visibility and escape responses. *Hydrobiol.* **292/293**,
417 447-453. (DOI 10.1007/BF00229971)
- 418 24. Titelman, J. & Kiørboe, T. 2003. Predator avoidance by nauplii. *Mar. Ecol. Prog. Ser.*
419 **247**, 137–149. (DOI 10.3354/meps247137)
- 420 25. Waggett, R. J. & Buskey, E. J. 2007. Copepod escape behavior in non-turbulent and
421 turbulent hydrodynamic regimes. *Mar. Ecol. Prog. Ser.* **334**, 193-198. (DOI
422 10.3354/meps334193)
- 423 26. Ohman, M. D. 1986. Predator-limited population growth of the copepod *Pseudocalanus*
424 sp. *J. Plankton Res.* **8**, 673–713. (DOI 10.1093/plankt/8.4.673)
- 425 27. Astroumoff, A. 1894. A Flying Copepod. *J. R. Microsc. Soc.* London. p618.
- 426 28. Zaitsev, Y. P. 1971. Marine neustonology. VA: National Marine Fisheries Service,
427 NOAA and National Science Foundation, National Technical Information Service.
- 428 29. Buskey, E. J. & Hartline, D. K. 2003. High speed video analysis of the escape responses
429 of the copepod *Acartia tonsa* to shadows. *Bio. Bull.* **204**, 28–37.
- 430 30. Vogel, S. 2005 Living in a physical world II. The bio-ballistics of small projectiles; *J.*
431 *Biosci.* **30** 167–175. (DOI 10.1007/BF02703696)
- 432 31. de Gennes, P. G., Brochard-Wyart, F. & Quéré, D. 2003. Capillarity and Wetting
433 Phenomena: Drops, Bubbles, Pearls, Waves. Springer, New York.
- 434 32. Turner, J. T., Tester, P. A. & Hettler, W. F. 1985. Zooplankton feeding ecology. *Mar.*
435 *Biol.* **90**, 1-8. (DOI 10.1007/BF00428208)
- 436 33. Govoni, J. J. & Grimes C. B. 1992. The surface accumulation of larval fishes by
437 hydrodynamic convergence within the Mississippi River plume front. *Cont. Shelf Res.* **12**,
438 1265–1276. (DOI 10.1016/0278-4343(92)90063-P)
- 439 34. Bonfil, R. 2009. The Biology and Ecology of the Silky Shark, *Carcharhinus Falciformis*,
440 in Sharks of the Open Ocean: Biology, Fisheries and Conservation (eds M. D. Camhi, E.
441 K. Pikitch and E. A. Babcock), Blackwell Publishing Ltd., Oxford, UK.
442 (DOI 10.1002/9781444302516.ch10)
- 443 35. Miller, T. J., Crowder, L. B. & Rice J. A. 1993. Ontogenetic changes in behavioural and
444 histological measures of visual acuity in three species of fish. *Environ. Biol. Fishes* **37**,
445 1–8. (DOI 10.1007/BF00000707)

- 446 36. Davenport, J. 1994. How and why do flying fish fly? *Rev. Fish Biol. Fisheries* **4**, 184–
447 214.
- 448 37. Saidel, W. M., Strain G. F. & Fornari S. K. 2004. Characterization of the Aerial Escape
449 Response of the African Butterfly Fish, *Pantodon buchholzi* Peters. *Environ. Biol. Fishes*
450 **71**, 63-72.
- 451 38. Strickler J. R. 1975. Swimming of planktonic *Cyclops* species (Copepoda, Crustacea):
452 Pattern, movements and their control. In Wu.T.Y.T., Brokaw. C. J. & Brennen. C. (eds),
453 *Swimming and Flying in Nature*. Plenum Press, Princeton, p613.
- 454 39. Alcaraz, M. & Strickler, J. R. 1988. Locomotion in copepods: patterns of movement and
455 energetic of *Cyclops*. *Hydrobiol.* **167/168**, 409-414. (DOI 10.1007/BF00026333)
- 456 40. Marrase, C., Costello, J. H., Granata, T. & Strickler, J. R. 1990. Grazing in a turbulent
457 environment: Energy dissipation, encounter rates, and efficacy of feeding currents in
458 *Centropages hamatus*. *Proc. Natl. Acad. Sci. USA* **87**, 1653-1657.
- 459 41. Hunt von Herbing, I. & Gallager, S. M. 2000. Foraging behavior in early Atlantic cod
460 larvae (*Gadus morhua*) feeding on a protozoan (*Balanion* sp.) and a copepod nauplius
461 (*Pseudodiaptomus* sp.). *Mar. Biol.* **136**, 591–602. (DOI 10.1007/s002270050719)
- 462 42. Becker, K., Hormchong, T. & Wahl, M. 2000. Relevance of crustacean carapace
463 wettability for fouling. *Hydrobiologia.* **426**, 193–201. (DOI 10.1023/A:1003918512565)
- 464 43. Ianora, A., Miralto, A. & Vanucci, S. 1992. The surface attachment structure: a unique
465 type of integumental formation in neustonic copepods. *Mar. Biol.* **113**, 401-407. (DOI
466 10.1007/BF00349165)
- 467 44. Blades, P. I. & Youngbluth, M. J. 1979. Mating behavior of *Labidocera aestiva*
468 (Copepoda: Calanoida). *Mar. Biol.* **51**, 339-355.

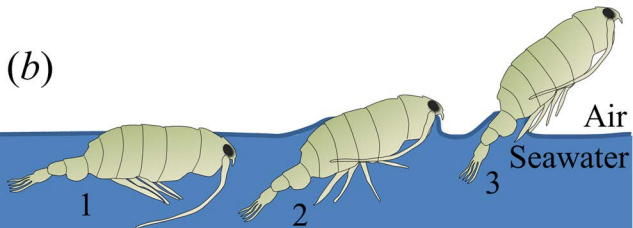




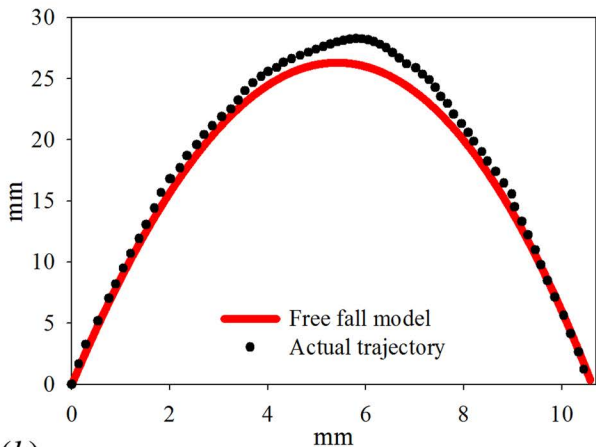
(a)



(b)



(a)



(b)

